Huang, Wei, Du, Jinxin, Yang, Xue-Xia, Che, Wenquan and Gao, Steven (2023)
A novel 24 GHz circularly polarised metasurface rectenna. IET Microwaves, Antennas & Propagation . ISSN 1751-8725.

ORIGINAL RESEARCH

The Institution of Engineering and Technology WILEY

A novel 24 GHz circularly polarised metasurface rectenna

Wei Huang[1] | Jinxin Du[2] | Xue-Xia Yang[1,3] | Wenquan Che[4] | Steven Gao[5]

[1]School of Communication and Information Engineering, Shanghai University, Shanghai, China

[2]Sino-European School of Technology, Shanghai University, Shanghai, China

[3]Key Laboratory of Specialty Fiber Optics and Optical Access Networks, Shanghai University, Shanghai, China

[4]School of Electronic and Information Engineering, South China University of Technology, Guangzhou, Guangdong, China

[5]University of Kent, Canterbury, UK

Correspondence

Xue-Xia Yang, School of Communication and Information Engineering, Shanghai University, Shanghai 200444, China.
Email: yang.xx@shu.edu.cn

Jinxin Du, Sino-European School of Technology, Shanghai University, Shanghai 200444, China.
Email: jinxin_du@shu.edu.cn

Funding information

National Natural Science Foundations of China, Grant/Award Numbers: 61931009, 62171270

Abstract

A novel 24 GHz circularly polarised metasurface rectenna for wireless power transmission is designed in this study. Based on experimental measurements and retro-simulation, an effective approach is proposed to extract the parasitic parameters of a Schottky diode. A highly efficient millimetre wave rectifier with a measured efficiency of 63% is constructed based on the exact equivalent circuit parameters of a diode. A circularly polarised metasurface antenna is adopted as the receiving antenna, and the gain is enhanced by introducing metal vias around the metasurface. The antenna and the rectifier are connected directly via a microstrip line. Measurements show that the metasurface antenna has a gain of 11.3 dBic and an axial ratio of 2.5 dB at 24 GHz. The measured conversion efficiency of the rectenna reaches 63% at 300 Ω load when the input power is 15.2 dBm. The rectenna has the advantages of low profile, which can be conformal to the electrical equipment.

KEYWORDS

equivalent circuits, millimetre wave antennas, millimetre wave diodes, rectennas, rectifying circuits

1 | INTRODUCTION

With the development of science and technology, the long-distance wireless power transmission (WPT) has been paid much attention in recent years [1, 2]. A WPT system consists of a transmitter and a receiver. The rectenna consists of a rectifying circuit and a receiving antenna, and can capture the electromagnetic wave and convert it into the direct current (DC) [3]. Both microwave and millimetre wave (mmW) can be used as energy carriers in WPT. In comparison, the mmW WPT system has the advantages of compact size, higher power capacity and better directivity [4, 5]. The mmW rectenna has been applied for 5G-powered IoT, wireless access and the wearable energy harvesting system [6–8].

The reported mmW-to-DC conversion efficiency of the rectifier is only 42% at 24 GHz which is below expectations in

Ref. [9]. One of the main reasons is the ambiguity or uncertainty of the parasitic parameters of the diode. In order to extract the parameters, a method based on a small signal S-parameter is proposed in Ref. [10], and the measured mmW-DC efficiency of the designed rectifier is 34% at 24 GHz. The similar method is used to extract parameters in Ref. [11], and a rectifying circuit is designed with the maximum efficiency of 67% at 35 GHz in Ref. [12]. However, the S-parameter curve varies with the magnitude of the input power. In other words, the extracted parameters from small signals S-parameters may not be applicable when the input power is much higher in actual work. By measuring the input impedance at different input powers and designing an impedance matching network to match the circuit, the rectifying circuit in Ref. [13] achieves a rectifying efficiency of 63% at 35 GHz. A tri-band rectifier with a multiband impedance matching network is presented in Ref. [14]; the

actual impedance of the rectifier is measured by using the through-reflect-line method. The maximum measured efficiencies at 24, 28, and 38 GHz are 44%, 41.3%, and 39.7% at an input power of 17.5 dBm. The drawback of the technique is that it is not generalisable since the impedance must be measured again when the structure of the rectifying circuit changes. To sum up, extracting the accurate parasitic parameters of the diode is of vital importance for designing high-efficiency rectifying circuits in mmW band.

The receiving antenna of a rectenna should have high gain to capture enough input power for rectification, such as the array antenna [15], the metallic waveguide Fabry-Perot antenna [16] and the enhanced Vivaldi antenna [17]. However, the complex feed network of the array antenna causes additional energy loss, the metallic antenna is bulky and heavy, and the Vivaldi rectenna is not conformal to the electrical equipment. Metasurface antennas have the advantages of a simple structure and low profile; it can be conformal to electrical equipments [18–20]. In addition, the use of circular polarisation wave is a solution to the polarisation alignment problem between the transmitter and receiver. Futhermore, only one set of rectifying circuits is required compared to the dual-polarised receiving antennas [21]. Designing a high-gain circularly polarised (CP) metasurface antenna is a good choice for the WPT system.

In this article, a novel 24 GHz CP metasurface rectenna with high rectifying efficiency is proposed. The rest of this paper is arranged as follows. In Section 2, the parasitic parameters of the MA4E1317 Schottky diode are extracted using a new method based on experimental measurements and retro-simulation, with an accurate equivalent model of the diode being achieved. Based on the precious equivalent parameters, a 24 GHz rectifying circuit is designed with the rectifying efficiency of 63% being measured. In Section 3, a low profile and high gain circularly polarised metasurface antenna is adopted as a receiving antenna. In order to further improve the gain, the metal vias structure around the metasurface is introduced into the periphery of the super surface. In Section 4, the metasurface antenna and the rectifying circuit are integrated to be a rectenna, whose maximum measured conversion efficiency reaches 63%.

2 | DESIGN AND MEASUREMENT OF THE RECTIFYING CIRCUIT

2.1 | Parameters of the Schottky diode

As a core component of the rectifier circuit, Figure 1a shows the 3D model of the diode. It contains two contact pads: a Schottky contact and a GaAs substrate. The diode is connected to the microstrip line by two contacts. The effect of the parasitic capacitor and parasitic inductance cannot be neglected in the mmW band. While these two parameters are unknown. Figure 1b shows the equivalent circuit model of a Schottky diode in which the unknown parasitic capacitor C_p and the parasitic inductor L_p is included, and the detailed extracted diode model parameters used in the harmonic

C_j	0.02 pF
R_S	4 Ω
V_{br}	7 V
V_{bi}	0.7 V
C_p	0.021 PF
L_p	0.067 nH
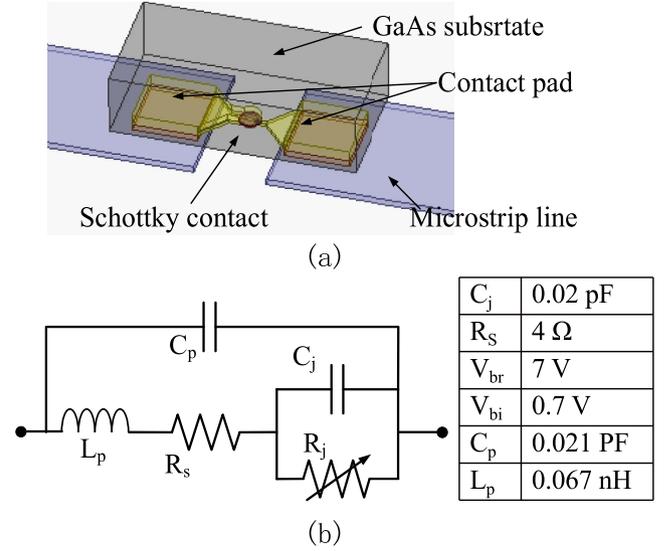
FIGURE 1 Equivalent circuit of Schottky diode: (a) 3D model of a Schottky diode, (b) Equivalent circuit

balance simulation is provided in a table format. The Schottky diode of type MA4E1317 is adopted in our work. Its highest operating frequency reaches 80 GHz, the zero-bias capacitance C_j is 0.02 pF, the built-in resistance R_S is 4 Ω, the reverse breakdown voltage V_{br} and positive lead forward voltage V_{bi} is 7 and 0.7 V, respectively. The junction resistance R_j will vary with the voltage at both ends of the diode. The cutoff operating frequency of the diode is determined by the zero-bias junction capacitance and the junction resistance. Higher rectifying efficiency can be achieved using diodes with a lower junction capacitance and resistance.

In order to extract parasitic parameters of the diode, a new method is suggested based on experimental measurements and retro-simulation of output voltage and rectifying efficiency. The procedure is as follows:

(1) Design a DC-pass filter to suppress the diode harmonics and design a rectifying circuit without an impedance matching network.
(2) Measure the input impedance of the unmatched circuit at different input power using an Agilent N5247A Vector Network Analyser.
(3) Design a 50 Ω impedance matching network to the measured input impedance, with a complete rectifying circuit being obtained.
(4) Measure the DC output voltage and rectifying efficiency of the rectifying circuit under various input power and load conditions.
(5) Create an equivalent circuit of the rectifying circuit in advanced design system (ADS) based on the size of the complete rectifying circuit and the Schottky diode equivalent circuit and set an initial parasitic parameter, C_p and L_p.
(6) Simulate the equivalent rectifying circuit by the harmonic balance method and S-parameter analysis in ADS, and then obtain the simulation DC output voltage and circuit rectifying efficiency at different input power and load.

(7) Compare the simulation and measurement data and set the values of C_p and L_p. If the simulation results agree with the test results, the actual parasitic parameters are extracted.

The parasitic capacitor is $C_p = 0.021$ pF, and the parasitic inductance is $L_p = 0.067$ nH. The data of this scheme is measured at a high input power, which is more suitable for the actual work.

2.2 | Design of 24 GHz rectifying circuit

The Schottky diode parasitic parameters are acquired and then a accurate diode equivalent model can be derived. With the help of the diode model, a 24 GHz rectifying circuit is designed using the harmonic balance method and large signal S-parameter analysis. Figure 2 shows the setup diagram of the ADS simulation circuit. Its structure is shown in Figure 3. The rectifying circuit consists of a MA4E1317 diode, an impedance matching network and a DC-pass filter. A quarter-wavelength microstrip line transformer is used to transfer the diode impedance to 50 Ω. Due to the non-linearity of diodes, higher harmonics are generated when mmWave signals pass through the diodes. The DC-pass filter between the diode and the load can keep the output DC voltage stable. The filter is composed of two fan-shape branches of radius R_1 and R_2 and an open-circuit stubs structure with length l_3, which is used to suppress the fundamental, second and third order harmonics, respectively. The DC-pass filter has good harmonic suppression performance, as shown by the S parameter in Figure 4. The attenuation is up to 30 dB at 24 GHz, 48 and 72 GHz. The rectifying circuit is fabricated on a TaconicTLY-5 dielectric substrate, with a thickness of 0.254 mm, a relative permittivity of 2.2 and a loss tangent of 0.0009.

The dimensions of the rectifying circuit are: $l_1 = 2.95$ mm, $l_2 = 2.3$ mm, $r_1 = 1.7$ mm, $r_2 = 0.8$ mm, $w_f = 0.78$ mm and $w_1 = 0.4$ mm.

2.3 | Simulated and measured results of the rectifying circuit

The setup for measuring the rectifying efficiency of the proposed rectifying circuit is shown in Figure 5. An Agilent E8257D mmW power source provides radio frequency power for the rectifying circuit. The output end of the rectifying circuit is connected with the DC load (resistor box), and the output voltage across the load can be measured by a voltmeter.

The rectifying efficiency of the rectifying circuit (η_c) is calculated according to Formula (1):

$$\eta_c = \frac{P_{DC}}{P_{mmW}} = \frac{V_{out}^2/R_L}{P_{mmW}} \times 100\%$$

where V_{out} is the output voltage, R_L is the DC load and P_{mmW} is the input power.

The measured and simulated results of the rectifying circuit at 24 GHz are indicated in Figure 6. Figure 6a shows that the measured rectifying efficiency reaches the maximum of 63% when P_{mmW} is 15 dBm and R_L is 300 Ω, and the measured output DC voltage is up to 2.5 V. The output voltage increases
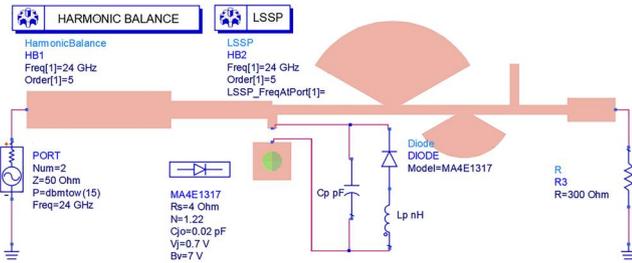
FIGURE 2 Setup diagram of ADS simulation circuit. ADS, advanced design system.
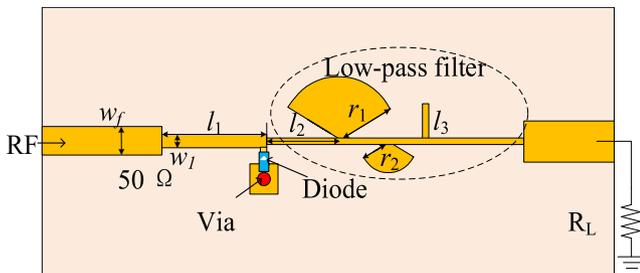
FIGURE 3 Structure of the 24 GHz rectifying circuit.
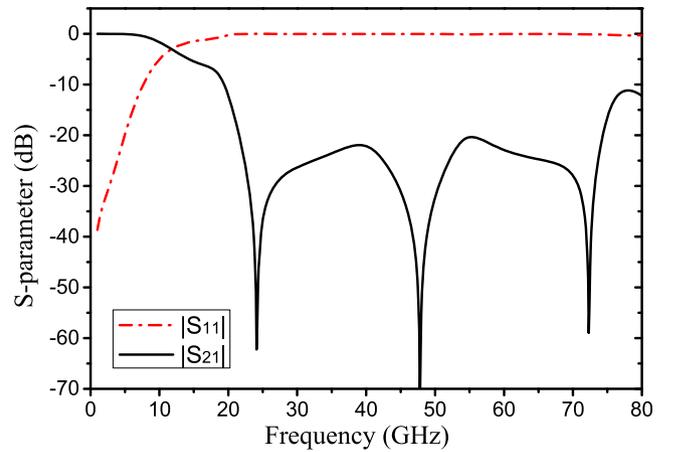
FIGURE 4 S-parameter of the DC-pass filter.
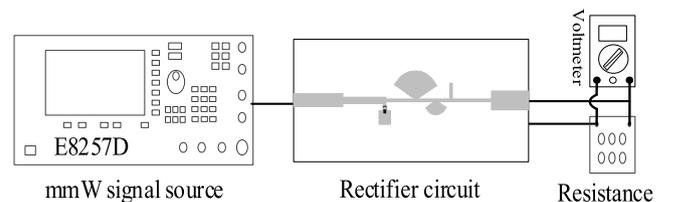
FIGURE 5 Measurement setup for the rectifying circuit.
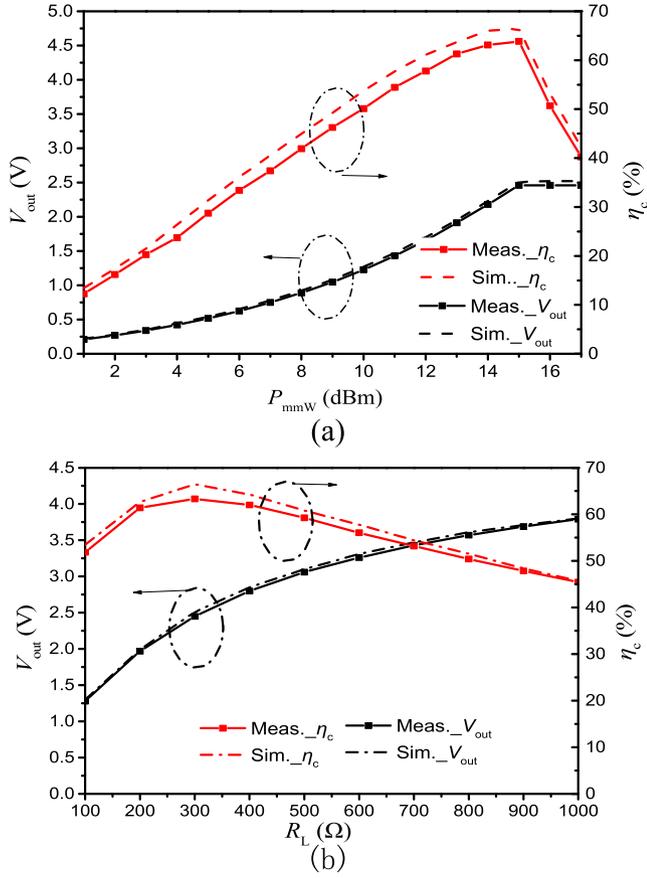
FIGURE 6 Measured and simulated results of the rectifying circuit at 24 GHz: (a) V_{ogt} and i_{ce} versus input power when load is 300 Ω, (b) V_{out} and η_c versus load with input power is 15 dBm

with the load, and the efficiency reaches the maximum when load is 300 Ω, as shown in Figure 6b. The measurement results are in good agreement with the simulation results. The accuracy of the extracted parasitic parameters is verified, and the method is effective.

To further illustrate the effect of parasitic parameters on the simulation results of the circuit, Figure 7 shows the rectifier circuit S parameters with and without parasitic parameters, when the load is 300 Ω and the input power is 15 dBm. The results show that the circuit maybe mismatch in the operating band when the parasitic parameters are not taken into account.

3 | DESIGN AND MEASUREMENT OF THE RECEIVING ANTENNA

3.1 | Structure of CP metasurface antenna

A circularly polarised metasurface antenna with high gain is design, as shown in Figure 8. The antenna consists of two layers of dielectric substrates of type TLY-5 and three layers of metal. A microstrip feedline with 50 Ω characteristic impedance is on the bottom. A ground plane with two cross-slots is in the middle layer. The metasurface on the top layer is
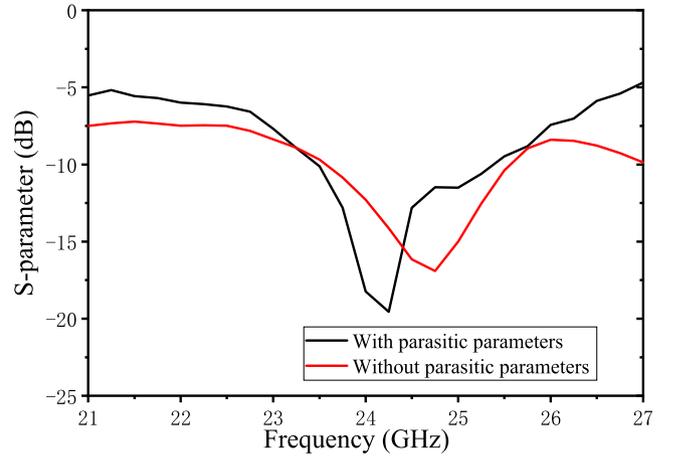
FIGURE 7 Measured S parameter results of the rectifying circuit when load is 300 Ω.
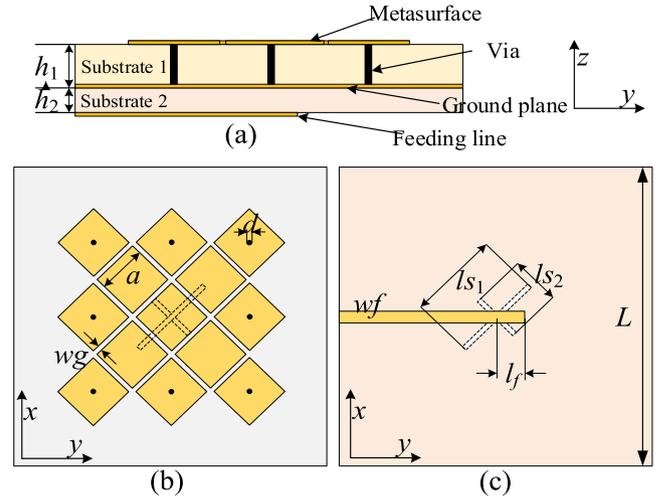
FIGURE 8 Geometry of the circularly polarised metasurface antenna: (a) Side view, (b) Top view, (c) Bottom view

composed of 13 square patches with the side length of a and inter-distance of w_g. Metal vias with a diameter of d are added in the centre position of the eight peripheral patches. The dimensions of the antenna are $a = 3$ mm, $w_g = 0.2$ mm, $L = 18$ mm, $w_f = 0.76$ mm, $l_f = 1.4$ mm, $d = 0.4$ mm, $ls_1 = 5.4$ mm, $ls_2 = 2.58$ mm, $h_1 = 0.51$ mm and $h_2 = 0.254$ mm.

3.2 | Simulated and measured results of receiving antenna

The operating frequency of the metasurface antenna is mainly determined by the side length a of the square patch and the inter-distance w_g, while the circular polarisation is achieved by cross-feeding slots of unequal lengths l_{s1} and l_{s2}. The axial ratio (AR) bandwidth and the input impedance of the antenna can be adjusted by changing the lengths of the cross slots and the

length of l_f. The simulated $|S_{11}|$ and AR of the proposed antenna with different a and w_g is shown in Figure 9. The operating frequency of the antenna shifts to lower frequency when a increases or w_g decreases. By adjusting these two parameters, the antenna can be tuned to operate at 24 GHz.

The gain can be increased by introducing metal vias at the centres of the eight side metasurface cells. Figure 10 shows the simulated gain of the metasurface antenna with and without via holes. It can be seen that the introduction of vias increases the gain by 1.5 dB. The simulated and measured antenna gains are 11.5 dBic and 11.3 dBic, respectively.

The metasurface antenna is prototyped and measured to verify the design. The $|S_{11}|$ and the axial ratio of the proposed antenna are shown in Figures 11 and 12. It can be seen that the antenna has a good impedance matching ($|S_{11}| < 10$ dB) in a broadband from 21.0 to 27.7 GHz, equivalent to a fractional bandwidth of 27.9% with respect to the central frequency. The measured 3-dB AR bandwidth is 12.8%, ranging from 21.7 to 25.1 GHz, and this band is fully overlap by the impedance bandwidth. Measured and simulated gains in various pitching angles θ are shown in Figure 13. The half power beamwidth is more than $\pm 50°$ in the xoz and yoz plane. The measured radiation patterns is consistent with the simulation.

4 | RECTENNA MEASUREMENTS

The receiving antenna and the rectifying circuit are usually connected through a connector. The feeding layer of the receiving antenna and the rectifying circuit adopt the same dielectric substrate in this article, and their terminals are all 50 Ω microstrip line; so the rectifying circuit and the metasurface antenna can be printed on opposite sides of two substrates to form a low-profile rectenna of 0.06 λ_0 thickness, and the ground plane with two cross-slots is in the middle layer. Figure 14 shows the photograph of the proposed metasurface rectenna.

The measurement system of the metasurface rectenna is shown in Figure 15. Agilent E8257D signal generator feeds the 24 GHz signal to the Ceyear 3871EC power amplifier, which transmits the mmW power through the horn antenna into free space. The power amplifier has an operating frequency of 18–26.5 GHz, an adjustable gain of 0–50 dB, a saturation output power of 50 dBm, and the output power can be read through the display. The linearly polarised horn antenna has a gain of 21
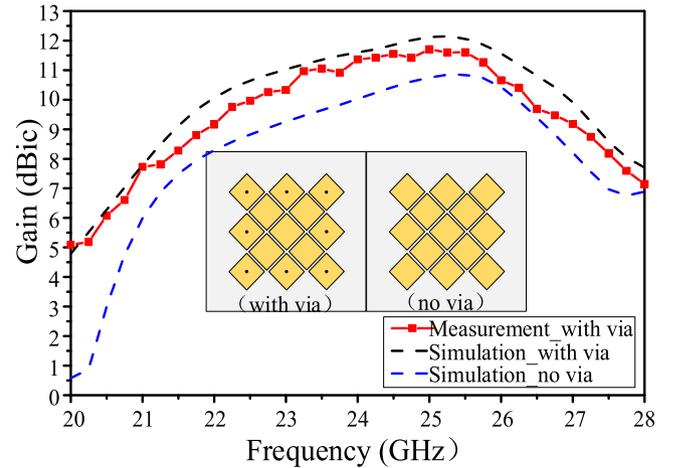
FIGURE 10 Gain of the metasurface antenna with and without vias.

FIGURE 9 Simulated $|S_{11}|$ and AR with: (a) different a, (b) different w_g
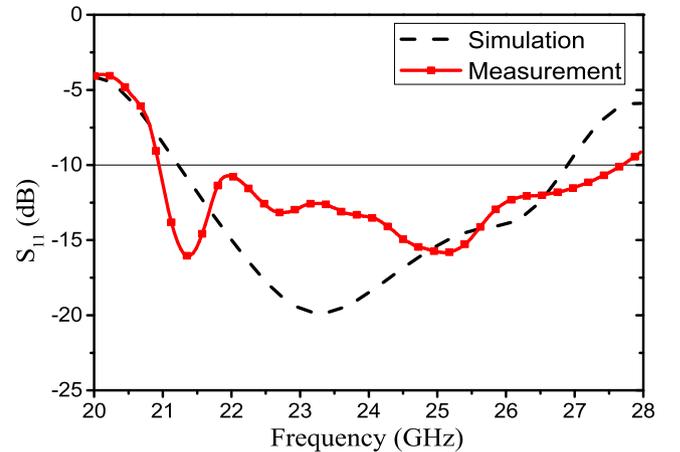
FIGURE 11 Reflection coefficients of the proposed metasurface antenna.
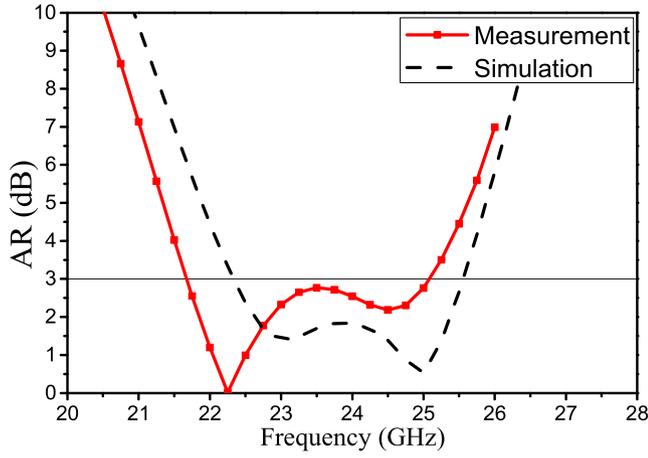
FIGURE 12 Axial ratio of the proposed metasurface antenna.
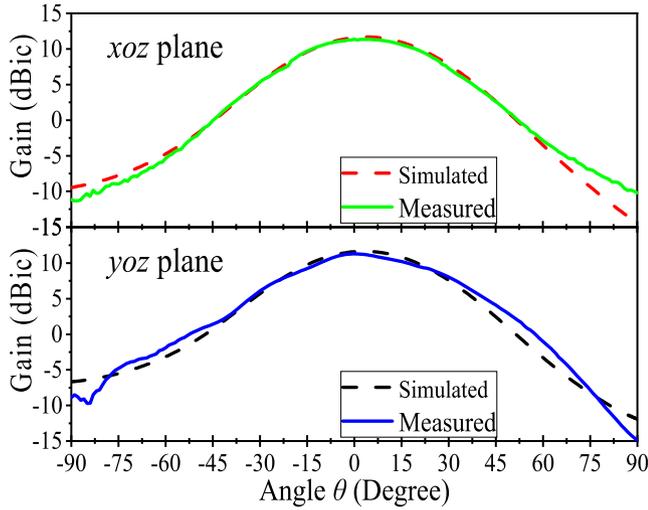
FIGURE 13 Gain of the proposed metasurface antenna various pitching angle θ.

dBi at 24 GHz. The receiver contains the rectenna, a resistance box and a DC voltmeter. The distance between the phase centres of the rectenna and the horn antenna is 69 cm to meet the far-field area ($\geq$56 cm). The rectenna is connected to the load (resistor box), and the DC voltage across the load is read from the voltmeter. The mmW-DC conversion efficiency of the rectenna is calculated according to Formula (2):

$$\eta_r = P_{DC}/P_{IN} \times 100\%$$

$$P_{DC} = V_{DC}^2/R_{Lr}$$

$$P_{IN} = P_t G_t G_r \lambda_0^2/(4\pi r)^2$$

where P_{DC} is the DC output power, R_{Lr} is the load at the rectenna output, V_{DC} is the DC voltage across the load, P_{IN} is the power captured by the rectenna, which can be calculated using the Friss transmission Formula (4), r is the distance
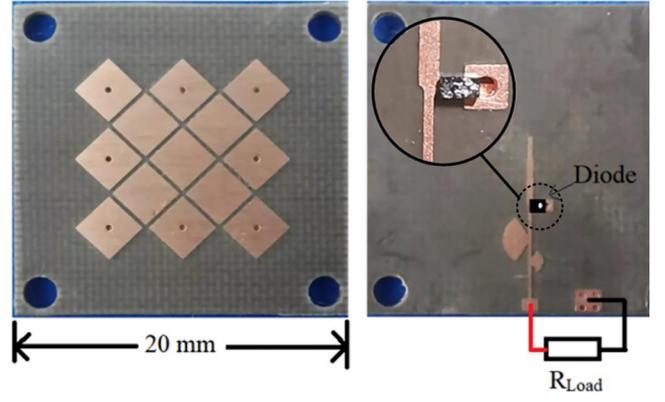
FIGURE 14 Top and bottom view of the proposed rectenna.
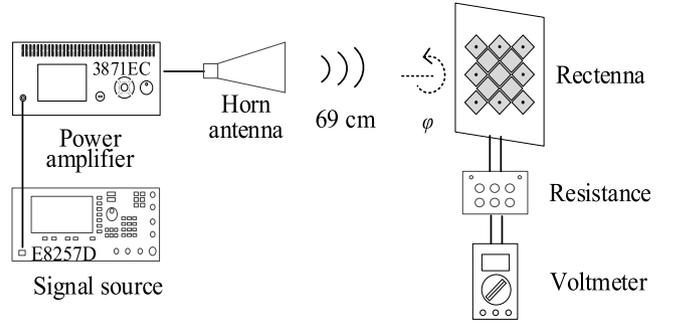
FIGURE 15 Measurement setup for the metasurface rectenna.

distance between phase centres of two antennas, P_t is the transmitted power and G_t is the gain of the transmitting horn antenna. It is worth noting that since the transmitting antenna is linearly polarised and the receiving antenna is circularly polarised, G_r must take the gain component of the corresponding polarisation, which in our case is 8.3 dBi.

The measured conversion efficiency and DC output voltage of the proposed rectenna versus loads and various input powers are depicted in Figure 16. According to Formula (4), the metasurface antenna received the power of 15.2 and 13.2 dBm at the transmission powers of 43 and 41 dBm. Among them, when the transmit power is set to 43 dBm, the DC load output voltage increases from 1 to 3.2 V with load changes from 50 to 1000 Ω, and the maximum MMW-DC conversion efficiency reaches 63% at 300 Ω. The measured conversion efficiency and DC output voltage of the proposed rectenna versus input powers on 300 Ω are listed in Figure 17. As the power received by the rectenna increases from 4 to 17 dBm, the DC output voltage continues to increase. When the rectenna receives 15.2 dBm of power, the conversion efficiency is maximised and the voltage is 2.51 V.

The measured conversion efficiency and the output DC voltage of the rectenna versus the frequency are shown in Figure 18; the resistive load is 300 Ω. The conversion efficiency reaches the maximum at 24 GHz. The measured bandwidth of the conversion efficiency over 30% is 3.5 GHz broadband (22.5–26 GHz). The transmit power is set to
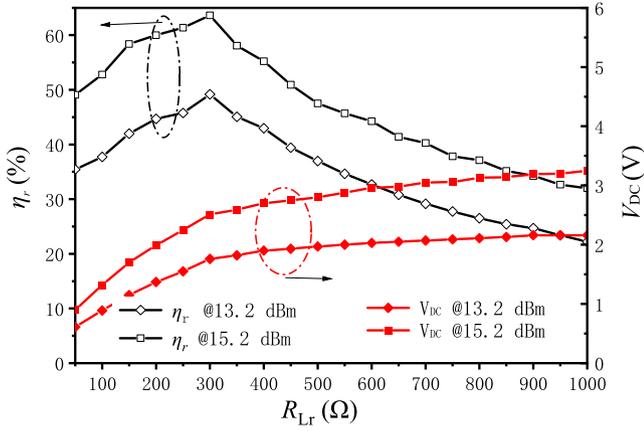
FIGURE 16 Measured conversion efficiency and output DC voltage of the proposed rectenna versus loads at various input powers.
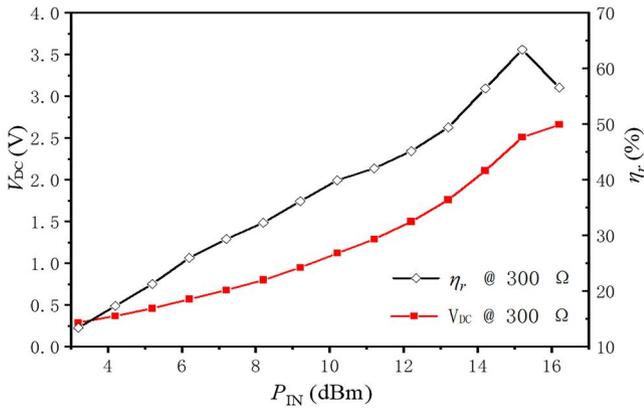
FIGURE 17 Measured conversion efficiency and output DC voltage of the proposed rectenna versus input powers.
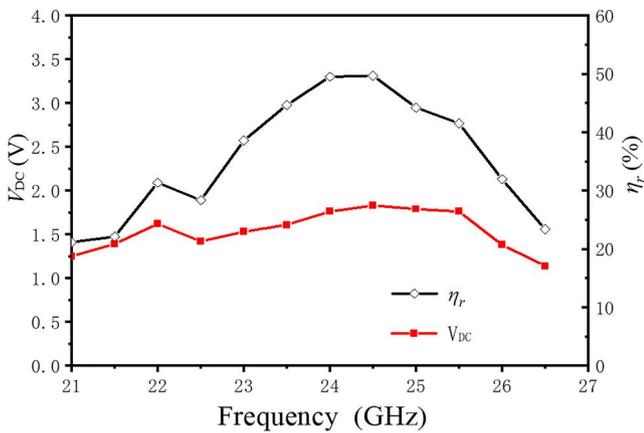
FIGURE 18 Measured V_{out} and conversion efficiency of rectenna versus the frequency.

41 dBm to prevent diode damage. When conversion efficiency is at its maximum, the input power is high and the diode is prone to reverse breakdown.
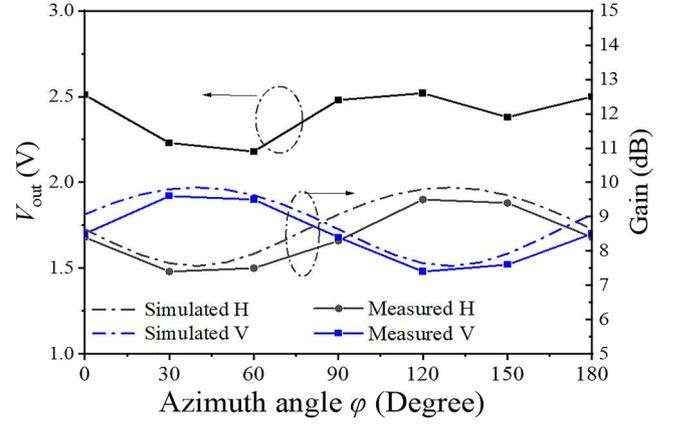
FIGURE 19 Measured V_{out} of rectenna and the measured and simulated gain components of vertical and horizontal versus azimuth angle φ.

In mobile applications, the polarisation direction for the rectenna is often unknown. When the rectenna is rotated around the normal direction, the DC output voltage changes in the range of 2.18–2.52 V with the azimuth angle φ changing from 0° to 180°, as shown in Figure 19, and the conversion efficiency is 48%–63% correspondingly. Also Figure 19 shows the measured and simulated gain components of vertical and horizontal. The transmitting horn is corresponding to the vertical component and as the gain of the vertical component becomes larger, the antenna receives more energy, which results in an increased output voltage. The output voltage fluctuated with the rotation angle θ, which might be caused by the measurement error, and the AR of the receiving antenna is not 0 dB at 24 GHz. The output voltage of the rectenna is stable with different input polarisation direction.

Table 1 shows the comparison of conversion efficiency between the designed rectenna and the published millimetre wave rectennas. The rectenna designed in this study has the highest efficiency compared to other rectennas operating at 24 GHz, and it has a more compact size.

5 | CONCLUSION

In this study, a new method for extracting the parasitic parameters of the diodes was proposed in the mmW band. The accurate equivalent circuit model of the MA4E1317 Schottky diode was created based on the extracted parasitic parameters, thereby a 24 GHz rectifying circuit was designed. The measured rectifying efficiency of the circuit reached 63% on a 300 Ω load when the input power is 15 dBm. A CP metasurface antenna with a high gain of 11.3 dBic has been proposed as the receiving antenna. The rectifying circuit and metasurface antenna have been integrated into a rectenna, and the measured highest conversion efficiency is 63%. The proposed CP metasurface rectenna has the characteristics of high conversion efficiency and low profile and can be conformal to the electrical equipment. It is suitable for the millimetre-wave power transmission system.

TABLE 1 Comparison among previous designed high frequency rectennas

	Operating frequency (GHz)	Receiving antenna	Area ($L \times W$, mm^2)	Gain	Maximum efficiency (%)
[8]	24	Antipodal Vivaldi antenna	32.6×16	8 dBi	12
[9]	24	2×2	40×55	12.6 dBic	24
[13]	35	2×2	30×18	14.7 dBi	60.9
[15]	35	4×4	22×42	19 dBi	67
This work	24	Meta-surface	20×20	11.3 dBic	63

AUTHOR CONTRIBUTIONS

Wei Huang: Conceptualisation; Data curation; Writing – original draft. **Jinxin Du:** Methodology; Writing – review & editing. **Xue-Xia Yang:** Project administration; Resources; Supervision; Writing – review & editing. **Wenquan Che:** Project administration; Supervision. **Steven Gao:** Formal analysis; Resources.

ACKNOWLEDGEMENT

CONFLICT OF INTEREST

We declare that we have no conflict of interest.

DATA AVAILABILITY STATEMENT

The data that support the findings of this study are available from the corresponding author upon reasonable request.

ORCID

Wei Huang https://orcid.org/0000-0003-2148-0704

REFERENCES

1. Shinohara, N.: Rectennas for microwave power transmission. IEICE Electron. Express 10(21), 1–13 (2013)
2. Yu, F., Yang, X.X.: Progress of rectenna arrays for microwave power transmission systems. Adv. Astronautics Sci. Technology 5, 1–10 (2022). https://doi.org/10.1007/s42423-022-00100-0
3. Wagih, M., Weddell, A.S., Beeby, S.: Rectenna for radio-frequency energy harvesting and wireless power transfer: a review of antenna design. IEEE Antennas Propag 62(5), 95–107 (2020). https://doi.org/10.1109/map.2020.3012872
4. Mei, H., et al.: High-efficiency microstrip rectenna for microwave power transmission at ka band with low cost. IET Microw., Antennas Propag. 10(15), 1648–1655 (2016). https://doi.org/10.1049/iet-map.2016.0025
5. Wagih, M., Weddell, A.S., Beeby, S.: Millimeter-wave power harvesting: a review. IEEE Open J. Antennas Propag 1, 560–578 (2020). https://doi.org/10.1109/ojap.2020.3028220
6. Shinohara, N., et al.: Development of 24 GHz rectenna for fixed wireless access. In: Conf. URSI General Assembly and Scientific Symposium, Istanbul, Turkey (2011)
7. Eid, A., Hester, J., Tentzeris, M.M.: A scalable high-gain and large-beamwidth mm-wave harvesting approach for 5G-powered IoT. In: Conf. 2019 IEEE MTT-S International Microwave Symposium (IMS), Boston (2019)
8. Wagih, M., et al.: BroadBand millimeter-wave textile-based flexible rectenna for wearable energy harvesting. IEEE Trans. Microw. Theor. Tech. 68(11), 4960–4972 (2020). https://doi.org/10.1109/tmtt.2020.3018735
9. Ladan, S., Guntupalli, A.B., Wu, K.: A high-efficiency 24 GHz rectenna development towards millimeter-wave energy harvesting and wireless power transmission. IEEE Trans. Circuits Syst. Regular Pap. 61(12), 3358–3366 (2014). https://doi.org/10.1109/tcsi.2014.2338616
10. Ladan, S., Wu, K.: Nonlinear modeling and harmonic recycling of millimeter-wave rectifying circuit. IEEE Trans. Microw. Theor. Tech. 63(3), 937–944 (2015). https://doi.org/10.1109/tmtt.2015.2396043
11. Chen, Q., et al.: Schottky diode large-signal equivalent-circuit parameters extraction for high-efficiency microwave rectifying circuit design. IEEE Trans. Circuits Syst. Express Briefs 67(11), 2722–2726 (2020). https://doi.org/10.1109/tcsii.2020.2977076
12. Chen, Q., et al.: A waveguide-fed 35- GHz rectifier with high conversion efficiency. IEEE Microw. Wirel. Compon. Lett. 30(3), 296–299 (2020). https://doi.org/10.1109/lmwc.2020.2968237
13. Wang, Y., et al.: Study on millimeter-wave siw rectenna and arrays with high conversion efficiency. IEEE Trans. Antennas Propag. 69(9), 5503–5511 (2021). https://doi.org/10.1109/tap.2021.3060120
14. Riaz, A., et al.: A triband rectifier toward millimeter-wave frequencies for energy harvesting and wireless power-transfer applications. IEEE Microw. Wirel. Compon. Lett. 31(2), 192–195 (2021). https://doi.org/10.1109/lmwc.2020.3037137
15. Mavaddat, A., Armaki, S.H.M., Erfanian, A.R.: Millimeter-wave energy harvesting using 4×4 microstrip patch antenna array. IEEE Antennas Wirel. Propag. Lett. 14, 515–518 (2015). https://doi.org/10.1109/lawp.2014.2370103
16. Chen, Q., et al.: A metallic waveguide-integrated 35- GHz rectenna with high conversion efficiency. IEEE Microw. Wirel. Compon. Lett. 30(8), 821–824 (2020). https://doi.org/10.1109/lmwc.2020.3002163
17. Tan, G.N., et al.: Study on millimeter-wave vivaldi rectenna and arrays with high conversion efficiency. Int. J. Antennas Propag 2016, 1–8 (2016). https://doi.org/10.1155/2016/1897283
18. Lin, F.H., Chen, Z.N.: Low-profile wideband metasurface antennas using characteristic mode analysis. IEEE Trans. Antennas Propag. 65(4), 1706–1713 (2017). https://doi.org/10.1109/tap.2017.2671036
19. Juan, Y., Yang, W., Che, W.: Miniaturized low-profile circularly polarized metasurface antenna using capacitive loading. IEEE Trans. Antennas Propag. 67(5), 3527–3532 (2019). https://doi.org/10.1109/tap.2019.2902735
20. Hussain, N., et al.: A metasurface-based low-profile wideband circularly polarized patch antenna for 5G millimeter-wave systems. IEEE Access 8, 22127–22135 (2020). https://doi.org/10.1109/access.2020.2969964
21. Sun, H., He, H., Huang, J.: Polarization-insensitive rectenna arrays with different power combining strategies. IEEE Antennas Wirel. Propag. Lett. 19(3), 492–496 (2020). https://doi.org/10.1109/lawp.2020.2968616